20th IMEKO TC4 International Symposium and
18th International Workshop on ADC Modelling and Testing
Research on Electric and Electronic Measurement for the Economic Upturn
Benevento, Italy, September 15-17, 2014

Estimation of quantum noise in fluoroscopy by analyzing differences of static images

P Bifulco[1], M Romano[1], M Cesarelli[1], L. Iuppariello[1], N Pasquino[1]

[1] *Department of Electrical Engineering and Information Technology (DIETI), University "Federico II" of Naples, Via Claudio, 21, 80125 Naples, Italy*

***Abstract* – Quantum noise is typical of images obtained with a small amount of photons and X-ray fluoroscopy is an example of the type. Indeed, to keep the doses of radiation to acceptable levels for the patient and, at the same time, to allow prolonged screening, the number of X photons is drastically reduced giving rise to a remarkable quantum noise on the images. For various applications it is necessary to estimate the level of this noise: this study proposes to use a limited number of fluoroscopic images depicting a static scene to estimate the noise. By considering the noise samples uncorrelated (e.g. for a single pixel) and computing all possible differences due to the number of images, it is possible to estimate fairly accurately the characteristics of the noise (and the gain of the sensor). Statistically, quantum noise is Poisson distributed, while the difference of two Poissonians gives a Skellam distribution. Making a difference between two static images will automatically result in cancellation of the image (the scene), whatever it is, highlighting only the noise. Using only few images it is possible to provide an estimation of noise, which is comparable (only slightly less accurate) to that should be obtained from an analysis performed with much more images.**

I. INTRODUCTION

Fluoroscopic images, widely used to support surgical and also diagnostic procedures, are characterized by a high level of noise due to the low dosage of X-rays involved. Use of low X-ray radiations is essential to reduce the dose to the patient, who needs to be exposed for long time (e.g. all the duration of the surgery). However, the availability of a low number of photons per pixel generates a peculiar and particularly intense noise in the fluoroscopic images: the so-called quantum noise (or photon statistical noise). Such noise exhibits a Poisson's statistics and represents the statistical imprecision caused by the random fluctuations in photon detection at the sensor. Since photon noise is inherent to the quantized nature of X-rays light, it gives a lower bound on the uncertainty of radiography measurements. This noise is intrinsic to the use of low level radiation, therefore it is unavoidable and it results dominant compared to all other sources of noise.

The number of photons K measured by a sensor element (e.g. a pixel) over a time interval T is described by the probability distribution [1,2,3,4]:

$$\Pr\left(K\big|_{\lambda,T}\right)=\frac{e^{-(\lambda T)}\cdot(\lambda T)^{K}}{K!}\quad;\quad \lambda T=\mu=\sigma^{2} \qquad (1)$$

where λ is the expected number of photons per unit time interval (radiation flux). The parameter (λT) of the Poisson distribution corresponds to the expected X-ray photon count, but also to the variance of photon count.

SNR of an image can be computed [5] as the ratio between the luminance of a pixel (mean) and the standard deviation of that pixel (SNR=μ/σ). It follows that the SNR varies as the square root of the luminance of the pixel. If the quantity λT exceeds the value of 10, as generally verified in practical fluoroscopy applications, Poisson distribution can be well approximated by a Gaussian distribution having a mean and variance both equal to the Poissonian mean:

$$P(\lambda T)\approx N(\lambda T,\lambda T) \qquad (2)$$

Generally, pixel intensity (i.e. luminance) is linearly dependent on the number of detected photons [6,7]. Therefore, saying G the detector gain, the luminance L of a pixel can be expressed as L = GλT. Therefore, the resulting statistical distribution of pixel luminance will show a mean of GλT and a variance of $G^2\lambda T$ (i.e. σ^2 = Gμ). Consequently, it can be well approximated by the Gaussian distribution $N(G\lambda T, G^2\lambda T) = N(L,GL)$.

It follows that, for a fluoroscopy image, the luminance will be linearly correlated to the variance of the noise.

The estimation of the relationship between the luminance (or the intensity or the grey-level of a pixel) and the noise variance is essential to fully characterize the quantum noise for a fluoroscopic image. The knowledge of this relationship is of paramount importance in many practical applications (e.g. noise filtering [8, 9, 10], dose reduction [11], edge detection [12,13], etc.). Fluoroscopic device is essential to track in real-time surgical instruments, catheters, wire guides inside patient's body supports angiography, angioplasty, pacemaker and defibrillator implantation, orthopaedic surgery, etc (e.g. [14,15]). Fluoroscopy also helps as diagnostic tool in analysis of the gastrointestinal tract, blood vessels, joints [6,16,17,18,19], implanted prosthesis [7].

ISBN-14: 978-92-990073-2-7

A practical way to obtain this estimate is to acquire a series of radiographic images of a static scene (taking care to include different grades of gray). In this manner, considered a generic pixel, the true degree of luminance can be estimated by calculating the time average of all the grey levels of that particular pixel. Then, calculating the standard deviation on the same data set (the time series of the grey level of a given pixel), is possible to estimate the variance of the noise associated to that pixel.

To obtain good estimates requires knowledge of a large number of samples and therefore it is necessary to record a series of images. Another way to obtain an equivalent estimate is to consider all the possible differences between the grey levels employed by a pixel using a reduced number of images.

At this point, it is important to analyze how a difference of Poisson random variables is distributed.

Difference D between two independent X-ray photon counts K1 and K2, each of them distributed as a Poisson, results a Skellam random variable, which is expressed as:

$$\Pr\left(D\big|_{\mu_1,\mu_2}\right) = e^{-(\mu_1+\mu_2)}\left(\frac{\mu_1}{\mu_2}\right)^{D/2} I_D\left(2\sqrt{\mu_1\mu_2}\right) \qquad (3)$$

where $\mu_1=\lambda_1 T_1$ and $\mu_2=\lambda_2 T_2$ are the expected values of the two Poisson distributions that were subtracted, while I_D is the modified Bessel function of the first kind [20].

The mean (μ_S) and the variance (σ_S^2) of a Skellam distribution depend on the parameters of the two Poisson distributions (4) and vice versa (5):

$$\begin{cases} \mu_S = \mu_1 - \mu_2 \\ \sigma_S^2 = \mu_1 + \mu_2 \end{cases} \quad (4) \qquad \begin{cases} \mu_1 = \dfrac{\mu_S + \sigma_S^2}{2} \\ \mu_2 = \dfrac{-\mu_S + \sigma_S^2}{2} \end{cases} \quad (5)$$

In the particular case (and also our case) in which $\mu_1 = \mu_2$ the expression of the Skellam distribution becomes:

$$\Pr\left(D\big|_{\mu_1=\mu_2=\mu}\right) = e^{-2\mu} I_D(2\mu) \qquad (6)$$

And therefore the mean is equal to zero while the variance is equal to 2μ.

The distribution Skellam is very well approximated by a normal or Gaussian distribution, having the same mean and variance of the Skellam. In case $\mu_1=\mu_2$ the approximation is:

$$S(0,2\mu) \approx N(0,2\mu) \qquad (7)$$

It turns out that, given a sequence of (uncorrelated) fluoroscopic images of a static scene, the variance of the Poisson noise can be measured by estimating the half variance of the correspondent Skellam distribution.

The purpose of this study is to evaluate the degree of approximation that can be achieved in the estimation of the noise parameters with a small number of fluoroscopic images of a static scene.

II. MATERIAL AND METHODS

In order to experimentally assess the degree of approximation of the model with real data, the estimation of the noise variance as a function of the mean pixel intensity from a real sequence of fluoroscopic static images was performed. To obtain actual data, real fluoroscopic image sequences of a motionless phantom were acquired by a fluoroscopic equipment.

The phantom by Nuclear Associates consists of an absorption material of increasing thickness so as to generate a ladder structure. This produces radiographic images consisting of stripes of different grey level. A GE OEC 9900 Elite fluoroscopic equipment, set to 52kVp and 28mA was employed. The size of each digital image was 1024 by 1024 pixels, while image intensity (luminance) had 16-bit precision. The fluoroscope was placed at 1 meter from the X-ray tube and the phantom was fixed as close as possible to the image intensifier. Digital images were acquired by the fluoroscope at a rate of 10 frames per second. A total of 80 images were acquired. The fluoroscopic sequence of images was processed using Matlab. The raw images gray levels were normalized to the range 0 (black)–1(white).

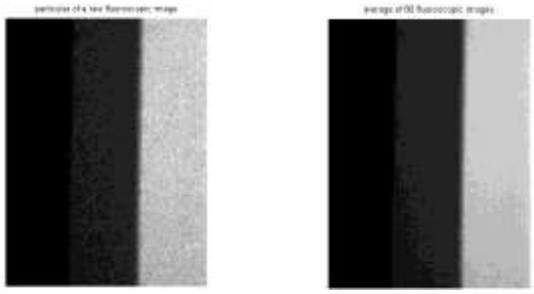

(a) (b)

Figure1: (a) particular of a raw (noisy) fluoroscopic image (step phantom). (b) Average (over time) of the full dataset of 80 images.

The fluoroscopic images were acquired with a time interval of a tenth of a second, this time is much longer than the image retention on the scintillator crystals and sensors (a few milliseconds). Therefore, the values assumed by a given pixel at different sampling time can be considered as independent samples. The entire time series of grey level values assumed by a given pixel was averaged to obtain an accurate estimate of the noise-free values (i.e. expected pixel intensity): so, a good estimate of the entire noise-free image was obtained. For the same time series was also computed the standard deviation, and, in turn, the variance of grey values assumed by a pixel. To estimate the relationship between the mean (luminance) and the variance of the quantum noise, linear regression was performed on data samples. This experimental linear relationship, obtained with a large number of images, was considered as a reference for the estimates that follows.

Small subsets of the acquired fluoroscopic images were considered; in particular, the subsets comprised a minimum of three to a maximum of twenty-five images.

Within a subset, all the possible, independent differences between images were computed pixel by

pixel. According to the above formulas, these values are samples of a Skellam distribution with zero mean and a variance double respect to that of the Poisson noise. Also the average of all the available values of the grey level of a pixel was computed in order to evaluate the relationship between the luminance and the noise variance each pixel.

Given a subset of N images, the number of all possible, independent, couple differences is given by the number of combinations of N objects in a group of size 2 (without repetition) $C_{N,2}$.

$$C_{N,2} = \binom{N}{2} = \frac{N!}{2!(N-2)!} \qquad (9)$$

Beside, the number of independent sampling of noise, on which to perform the average operation (to obtain the mean grey level of a pixel) is obviously N.

Similarly to the estimation of Poisson noise characteristics involving the whole fluoroscopic image dataset, grey levels (luminance) vs Skellam variances (for each pixel) were plotted and a linear regression was performed to estimate the linear relationship for each of the fluoroscopic image subset. Results were analyzed to highlight the degree of approximation of noise properties using only few fluoroscopic images of a static scene.

III. RESULTS

Fig. 2 represents the experimental data obtained using the full fluoroscopic image dataset, by computing, per each pixel, the average and the variance of the grey levels actually assumed. The linear regression line is also represented.

The angular (or alpha) coefficient of the straight line obtained can be considered as an estimate of the gain of the detector. As it is possible to note in Fig 2, the Y-intercept of the regression line resulted about zero, as expected. The coefficient of determination R^2 of the linear regression resulted almost equal to one: this represents a very good fitting of the experimental data.

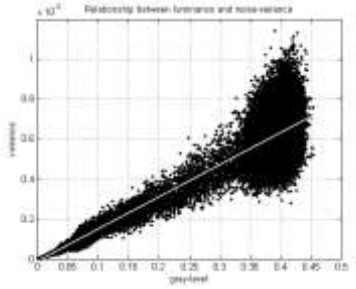

*Figure2: Estimated relationship between luminance and noise-variance (all images were processed). Experimental data are plotted as black dots. The regression (white) equation is: variance=0.00161*luminance-1.2e-005; the determination coefficient R^2=0.95*

Similarly to Fig. 2, as an example, Fig. 3 represents the experimental data obtained using a fluoroscopic image subset (comprising 15 images), by computing, per each pixel, the average of the grey levels and the variance of all the possible, independent differences.

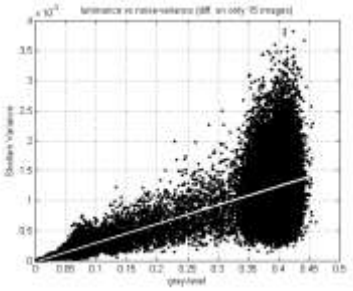

*Figure3: Estimated relationship between luminance and Skellam noise-variance (processing only the differences of 15 images). Experimental data (black dots). The regression line (white) equation is: variance=0,00325*luminance-2.4e-005; the determ. coefficient R^2=0.80*

Table 1 summarizes the results obtained by the estimation of the noise parameters with respect to the numerosity of the subsets considered.

N. imm.	alpha	beta	R^2
3	0,00413	<10-4	0,35
4	0,00368	<10-4	0,45
5	0,00350	<10-4	0,52
6	0,00343	<10-4	0,58
7	0,00338	<10-4	0,62
8	0,00335	<10-4	0,66
9	0,00332	<10-4	0,69
10	0,00330	<10-4	0,71
11	0,00329	<10-4	0,73
12	0,00328	<10-4	0,75
13	0,00327	<10-4	0,77
14	0,00326	<10-4	0,78
15	0,00325	<10-4	0,80
16	0,00325	<10-4	0,81
17	0,00324	<10-4	0,82
18	0,00324	<10-4	0,82
19	0,00324	<10-4	0,83
20	0,00324	<10-4	0,84
21	0,00324	<10-4	0,85
22	0,00323	<10-4	0,85
23	0,00323	<10-4	0,86
24	0,00323	<10-4	0,86
25	0,00323	<10-4	0,87

Table 1: values of the linear regression (alpha coefficient: noise-variance/luminance; beta: bias or Y-intercept of the regression straight line; R^2: coefficient of determination of the regression) obtained considering image subsets of different numerosity (N. imm.)

The following figures (4a, 4b and 4c) respectively represent: the estimate of the slope of the linear regression line (alpha coefficient); the percentage error on the estimate of the alpha coefficient; the values of the coefficient of determination R^2 of the linear regression versus the number of images considered.

IV. COMMENTS AND CONCLUSIONS

Analysis of the results provides a quantification of the approximation achievable by using a reduced number of fluoroscopic images of a static scene. By considering that the frame rate available in modern fluoroscopy devices can reach up to 30 fps, it follows that in less than a second is possible to acquire enough images to measure noise characteristics with an acceptable approximation. Appropriate knowledge of the parameters of the quantum noise is of paramount importance for the processing of fluoroscopic images. Noise reduction can improve image quality and in turn doctors' visual perception during operation or diagnosis.

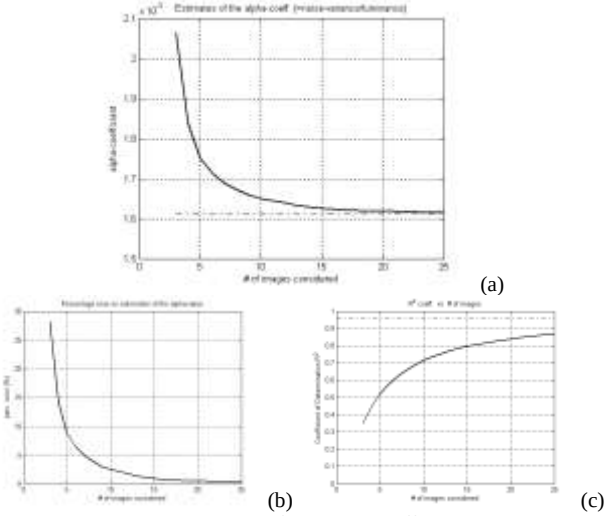

(a) (b) (c)

Figure4: (a) Estimates of the alpha coefficient (noise-variance/luminance) of the linear regression vs number of images; (b) Percentage error on the estimation of alpha coefficient vs # of images; (c) Values of the coefficient of determination R^2 vs # of images.

Also the operations of the image processing to highlight the contours of objects, such as surgical instruments or implants, may find great advantage in knowing the characteristics of the noise.

REFERENCES

[1] R.M. Harrison, C.J. Kotre, "Noise and threshold contrast characteristics of a digital fluoroscopic system," Physical in Medicine and Biology, vol.31, pp.512– 586, 1986.

[2] M.J. Tapiovaara, "SNR and noise measurements for medical imaging: II. Application to fluoroscopic X-ray equipment,". Physical in Medicine and Biology, vol.38, no.2, pp.1761–1788, 1993, doi:10.1088/0031-9155/38/12/006.

[3] C.L. Chan, A.K. Katsaggelos, A.V. Sahakian, "Image sequence filtering in quantum-limited noise with applications to low-dose fluoroscopy," IEEE Trans. Medical Imaging, vol.12, no.3, pp.610 621, 1993.

[4] M. Hensel, T. Pralow, A.V. Grigat, "Modeling and real-time estimation of signal-dependent noise in quantum-limited imaging," in Proc. WSEAS international conference on signal processing, robotics and automation, Corfu Island, Greece, 2007, pp. 183–191.

[5] Gonzalez RC, Woods RE (1992) Digital image processing, 3rd edition. Addison-Wesley, Reading, Massachusetts

[6] P. Bifulco, M. Cesarelli, T. Cerciello, M. Romano, "A continuous description of intervertebral motion by means of spline interpolation of kinematic data extracted by videofluoroscopy," Journal of Biomechanics, vol.45, no.4, pp.634-641, 2012, DOI:10.1016/j.jbiomech.2011.12.022.

[7] T. Yamazaki, T. Watanabe, Y. Nakajima, K. Sugamoto, T. Tomita, H. Yoshikawa, S. Tamura. "Improvement of depth position in 2-D/3-D registration of knee implants using single-plane fluoroscopy," IEEE Trans. on Medical Imaging, vol.23, no.5, pp.602-612, 2004, DOI: 10.1109/TMI.2004.826051.

[8] T. Cerciello, M. Cesarelli, L. Paura, P. Bifulco, M. Romano, R. Allen, "Noise-parameter modeling and estimation for X-ray fluoroscopy," in Proc. International symposium on applied sciences in biomedical and communication technologies, Barcelona, Spain, 2011, pp.1–5.

[9] M. Cesarelli, P. Bifulco, T. Cerciello, M. Romano, L. Paura, "X-ray fluoroscopy noise modeling for filter design," Int. J Comput Assist Radiol Surg, vol.8, no.2, pp 269-278, 2013. DOI: 10.1007/s11548-012-0772-8.

[10] T. Cerciello, P. Bifulco, M. Cesarelli, A. Fratini, "A comparison of denoising methods for X-ray fluoroscopic images," Biomedical Signal Processing and Control, vol.7, no.6, pp.550-559, 2012. DOI:10.1016/j.bspc.2012.06.004.

[11] Wang J, Zhu L, Xing L. Noise Reduction in Low-Dose X-Ray Fluoroscopy for Image-Guided Radiation Therapy. International Journal of Radiation Oncology Biology Physics. 2009; 74 (2) , pp. 637-643. DOI: 10.1016/j.ijrobp.2009.01.020

[12] P. Bifulco, M. Sansone, M. Cesarelli, R. Allen, M. Bracale, "Estimation of out-of-plane vertebra rotations on radiographic projections using CT data: a simulation study" Med Eng Phys, vol.24, no.4, pp.295–300, 2002. DOI: 10.1016/S1350-4533(02)00021-8

[13] P. Bifulco, M. Cesarelli, R. Allen, M. Romano, A. Fratini, G. Pasquariello, "2D-3D registration of CT Vertebra volume to fluoroscopic projection: a calibration model assessment" EURASIP J Adv Signal Process, vol.10, pp.1–8, 2010. DOI: 10.1155/2010/806094

[14] M. Moradi, S.S. Mahdavi, E. Dehghan, J.R. Lobo, S. Deshmukh, W.J. Morris, G. Fichtinger, S.E. Salcudean, "Seed localization in Ultrasound and Registration to C-Arm Fluoroscopy Using Matched Needle Tracks for Prostate Brachytherapy," IEEE Trans. on Biomedical Engineering, Vol.59, n°9, pp. 2558–2567, 2012, DOI: 10.1109/TBME.2012.2206808.

[15] J. Weese, G.P. Penney, P. Desmedt, T.M. Buzug, D.L.G. Hill, D.J. Hawkes, "Voxel-based 2-D/3-D registration of fluoroscopy images and CT scans for image-guided surgery," IEEE Trans. on Information Technology in Biomedicine, Vol.1, no.4, pp.284-293, 1997 DOI: 10.1109/4233.681173

[16] T. Cerciello, P. Bifulco, M. Cesarelli, L. Paura, G. Pasquariello, R. Allen, "Noise reduction in fluoroscopic image sequences for joint kinematics analysis," in Proc. Mediterranean conference on medical and biological engineering and computing, 2010, vol.29, pp.323–326. DOI: 10.1007/978-3-642-13039-7_81

[17] T. Cerciello, M. Romano, P. Bifulco, M. Cesarelli, R. Allen, "Advanced template matching method for estimation of intervertebral kinematics of lumbar spine" Medical Engineering Physics vol.33, no.10, pp.1293 1302, 2011. DOI: 10.1016/j.medengphy.2011.06.009

[18] P. Bifulco, M. Cesarelli, R. Allen, M. Sansone, M. Bracale, "Automatic recognition of vertebral landmarks in fluoroscopic sequences for analysis of intervertebral kinematics" J Med Biol Eng Comput, vol. 39, no.1, pp.65 75, 2001.

[19] P. Bifulco, M. Cesarelli, M. Romano, A. Fratini, M. Sansone. Measurement of intervertebral cervical motion by means of dynamic X-ray image processing and data interpolation. International Journal of Biomedical Imaging. Volume 2013, 2013, Article number 152920. DOI: 10.1155/2013/152920

[20] Skellam JG (1946) The frequency distribution of the difference between two poisson variates belonging to different populations. J R Stat Soc Ser A 109(3):296